EM Implosion Memos

Memo 18

September 2007

Experimental Setups and Comparison of the Experimental and Analytical Results for the Waveform of Two and Four-Feed Arms Prolate-Spheroidal IRA

Serhat Altunc , C. Jerald Buchenauer and Carl E. Baum

University of New Mexico
Department of Electrical and Computer Engineering
Albuquerque New Mexico 87131

Abstract

Experimental setups of two and four-feed arms prolate-spheroidal IRA are used to obtain better focusing for a prolate-spheroidal IRA. Analytical results are used for verification.

1 Introduction

This paper is a summary of experimental setups and the dimensions of this setup are based on [1,2]. This setup will be used for a biological application [3]. Experimental setup and problems related with measurements or devices are discussed.

We compare experimental and analytical results. We discuss the differences between these results and analyze the errors.

2 Analytical Calculation

At the second focus the calculated fields are as follows [1,2]

$$E_\delta = \frac{V_0}{\pi f_g c}\frac{a+c}{a-c}\cot\left(\frac{\theta_c}{2}\right)\left[1-\left[1+\left[\frac{\Psi_p}{z_0-z_p}\right]^2\right]^{-1/2}\right]$$

$$E_s = \frac{V_0}{2\pi f_g}\frac{1}{z_0-z_p}\frac{a+z_0}{a-z_0}\cot\left(\frac{\theta_c}{2}\right)\left[1+\left[\frac{z_0-z_p}{\Psi_p}\right]^2\right]^{-1} \qquad (1)$$

$$E_p = \frac{V_0}{2\pi f_g z_0}\tan\left(\frac{\theta_c}{2}\right),\ E_{p_2} = \frac{V_0}{2\pi f_g}\frac{1}{z_0}\frac{b}{a+z_0}\left[1+\left[\frac{z_0}{b}\right]^2\right]^{-1}$$

where E_δ and E_s are the impulsive and step terms from the reflection in the prolate sphere and E_p is the magnitude of the prepulse wave from first focus(valid up to the time of aperture truncation), E_{P2} is the prepulse term after the impulse, ie after the truncation at the aperture boundary

Our excitation is $V_0 = 0.5\,V$ (peak-peak 1 V) and has $t_\delta = 100\,ps$, rise time so for this excitation we have the focal waveforms as presented in fig.7.

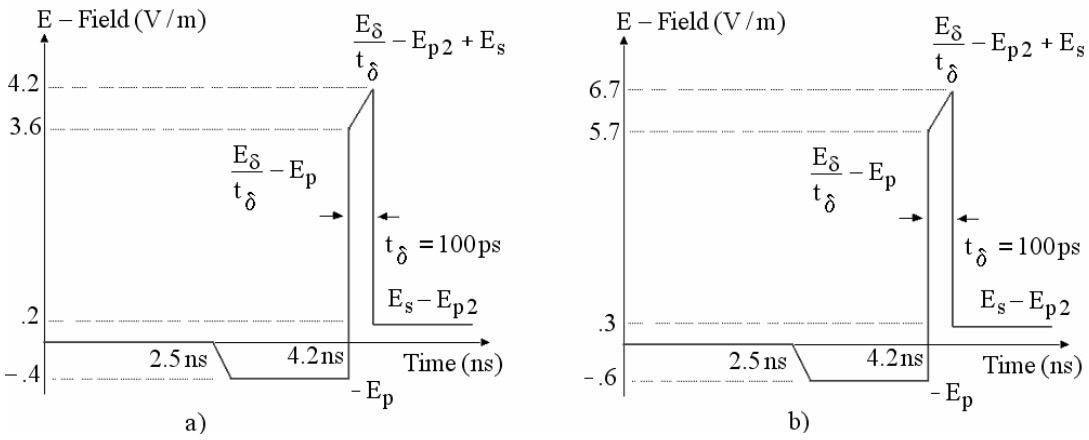

Figure 1: Analytical Focal Waveforms a)Two-Arm b) 60^o Four-Arms

We use maximum t_{mr} (based on maximum rate of rise) as t_{δ} to compare our experimental results with analytical results. For a step like $f(t)$, t_{mr} is

$$t_{mr} = \frac{f_{max}}{\left.\frac{df}{dt}\right|_{max}} \tag{2}$$

3 Experimental Setup and Data Analysis Technique

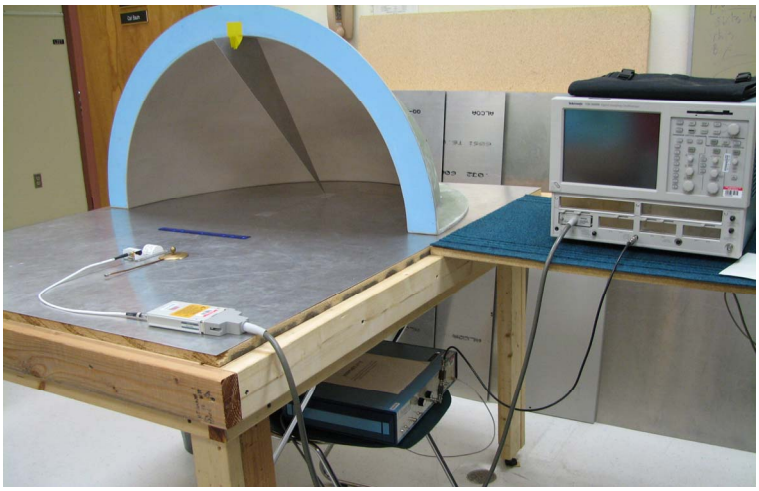

Figure 2: Experimental Setup for a Two-Feed Arms Prolate-Spheroidal IRA

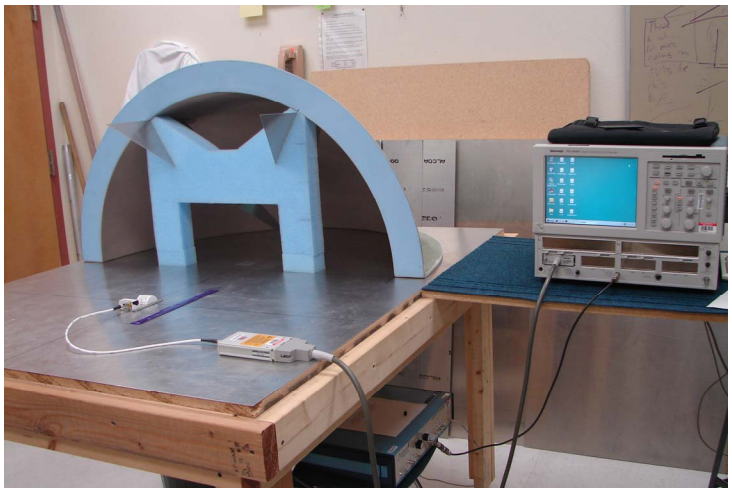

Figure 3: Experimental Setup for a 60^{o} Four-Feed Arms Prolate-Spheroidal IRA

The experimental setup basically includes three basic parts. These are a prolate-spheroidal reflector with feed arms, a sampling-oscilloscope and a pulse generator and they are presented in figs.2 and 3.

Figure 4: Sampling-Oscilloscope and Pulse Generator

One can see from fig. 4 that we use a Tekronix TDS 8000B Digital Sampling-Oscilloscope to measure the waveform at the second focal point. A Picosecond Pulse Labs Pulse generator is used for excitation.

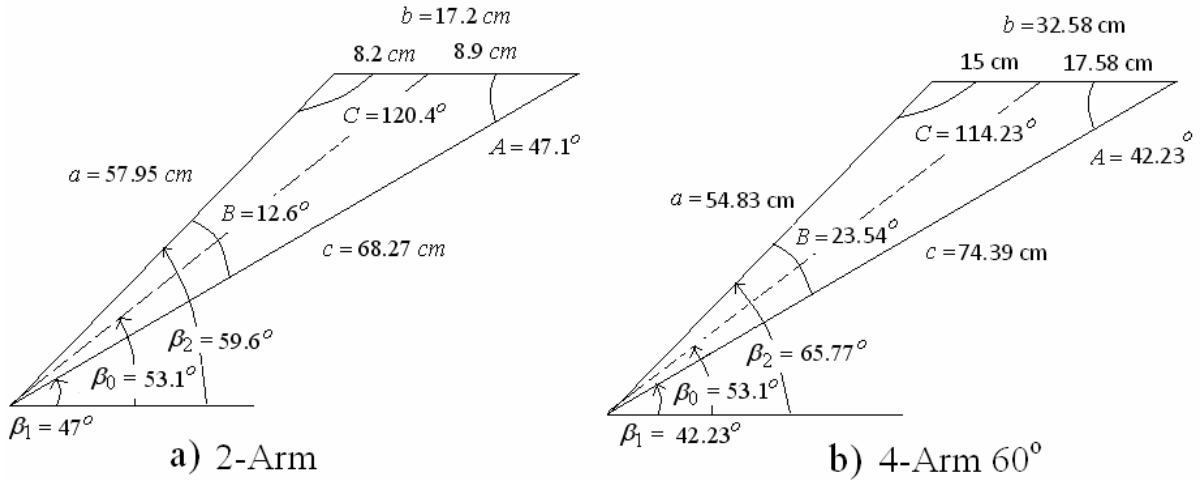

Figure 5: Two-Feed Arms and 60^o Four-Feed Arms Dimensions

In fig.5 feed arms dimensions are calculated in [2]

One can see four 60^o feed arms in fig.5 and it is located in the reflector . We use foam which has a relative dielectric constant $\varepsilon_r = 1.013$ to hold the feed arms angle as 60^o .

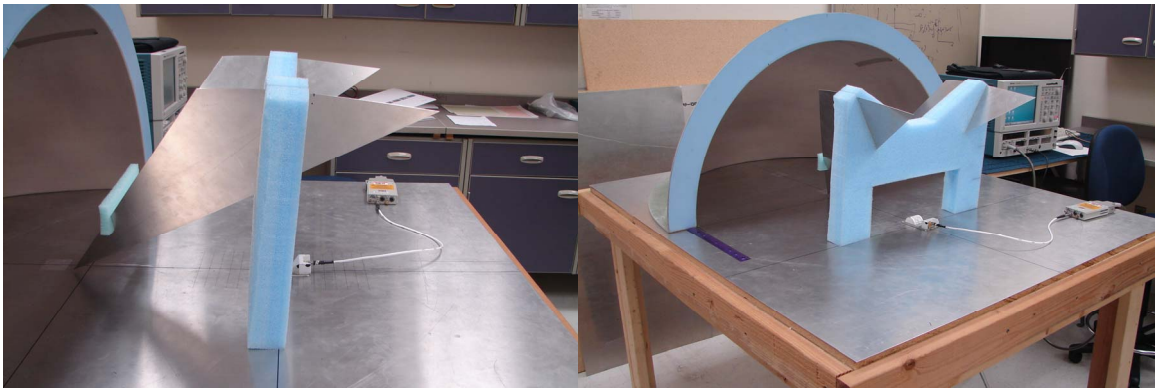

Figure 6: 60^{o} Four-Feed Arms

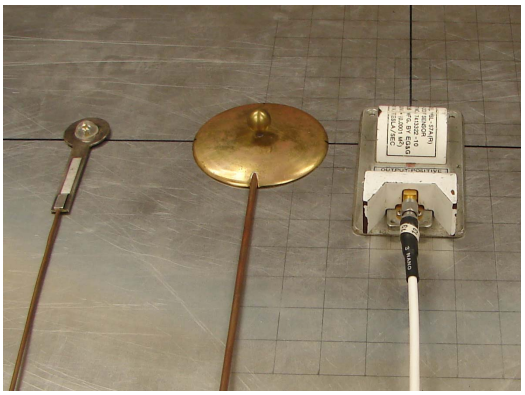

Figure 7: Fast D-Dot, Slow D-Dot and B-Dot Probe

One can see Fast D-Dot, D-Dot and B-Dot probes in fig.6. We use the B-Dot probe to get the magnetic field and calibrate D-Dot data with the prepulse data of the B-Dot probe. We use the data from B-dot probe which has an equivalent area $A_{eq} = 1cm^2$ and analyze the data as follows

$$V = A_{eq} \frac{dB}{dt}$$
$$B = \frac{1}{A_{eq}} \int_{-\infty}^{t} V(t')\, dt' \qquad (3)$$

So we can find equivalent E-field as

$$E_{eq} = cB = \frac{c}{A_{eq}} \int_{-\infty}^{t} V(t')dt' \qquad (4)$$

This equivalent E-field E_{eq} gives the exact result for the prepulse because we have a TEM wave and $E/H = \eta_0 = 376.7\Omega$ for free space. We calibrate our D-Dot data with comparing prepulse term.
We export data for D-Dot probe and analyze the data as follows

$$I = \frac{V}{Z_0} = A_{eq}\frac{dD}{dt}$$
$$E = \frac{1}{\varepsilon_0 Z_0 A_{eq}}\int_{-\infty}^{t} V(t')\,dt' \tag{5}$$

Our pulse generator has a $V_0 = 10\,V$ excitation so we feed our IRA with

$$V = T\,V_0 \tag{6}$$

Where T is the transmission coefficient

$$T = \frac{2Z_L}{Z_L + Z_0} \tag{7}$$

The pulse impedances for the two-arm and four 60^o feed arm cases are 400Ω and 200Ω. We have a ground plane so $Z_L = 200\Omega$ *and* 100Ω. The transmission coefficients are 1.6 and 1.33. In our analytical calculation we use $V_0 = 0.5\,V$ so we can normalize the data to get the E-field as

$$E_N = \frac{1}{20T\,\varepsilon_0 Z_0 A_{eq}}\int_{-\infty}^{t} V(t')\,dt \tag{8}$$

3.1 Experimental Results

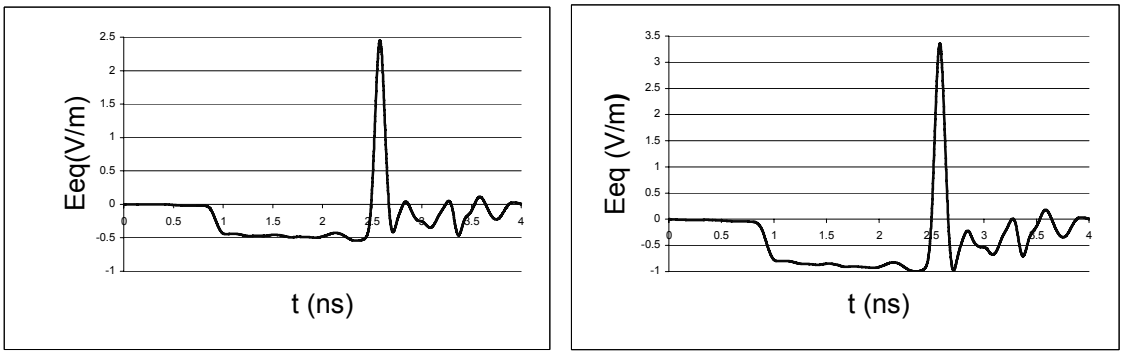

Figure 8: B-Dot Probe Focal Waveforms Two-Arms and 60^o Four-Feed Arms

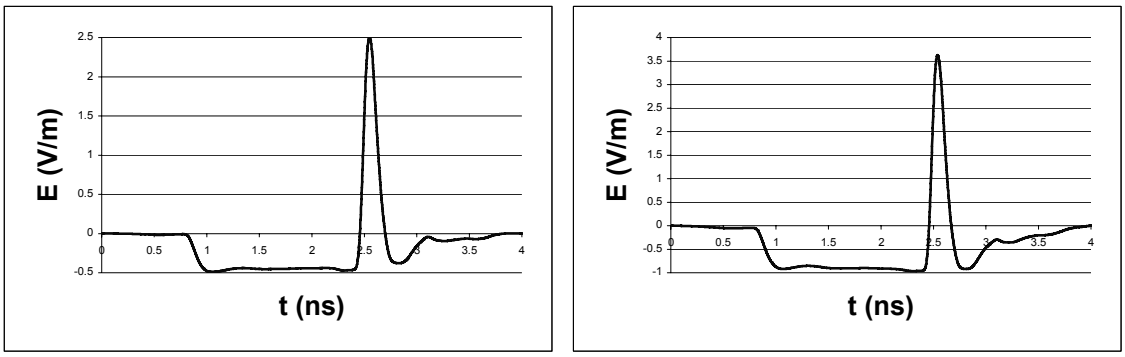

Figure 9: Slow D-Dot Probe Focal Waveforms Two-Arms and 60^{o} Four-Feed Arms

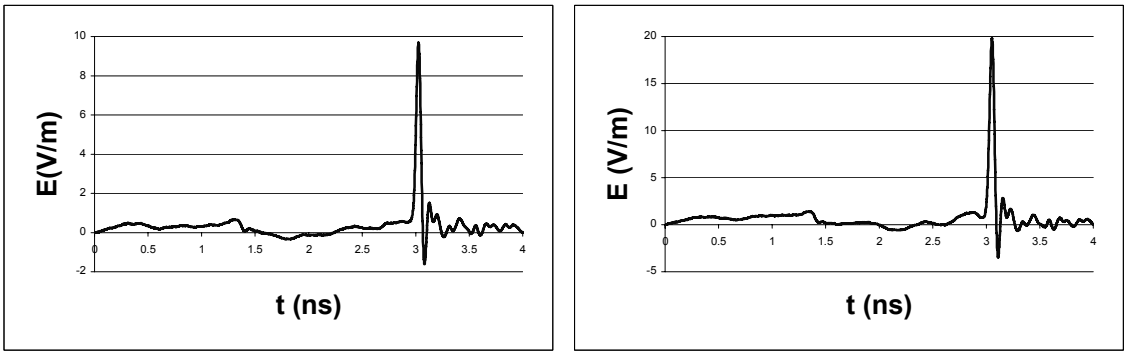

Figure 10: Fast D-Dot Probe Focal Waveforms Two-Arms and 60^{o} Four-Feed Arms

One can see from fig.8 and 9 the results are close but for slow D-Dot sensor we do not have that much oscillation in the postpulse so they have different frequency response we have more bandwidth limitation for slow D-Dot sensor. One can see in fig.10 that if we use the fast D-Dot sensor we have this oscillation so the oscillation are not due to different type of sensors.

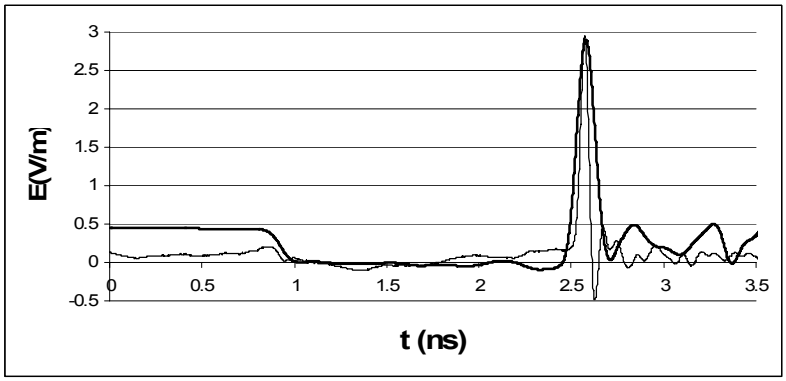

Figure 11: Focal Waveform for B-Dot and Normalized Focal Waveform for Fast D-Dot of a Two-Arm IRA

One can compare Focal Waveform for B-Dot and Normalized Focal Waveform for Fast D-dot. They are oscillating in different frequencies fast D-Dot sensor is too fast this can cause errors in postpulse. We do not have ringing in the slow D-Dot, we think our B-Dot sensor causes around

3 GHz ringing. There will always be causes for oscillations and aberrations at the levels observed in the fast D-dot trace. There are cable and connection non uniformities, nonlinear effects in the sampler, sampling time errors, digitizing errors, etc. Most importantly, the generator signal is not pure and has lots of aberrations after the step. These can be removed numerically, but if pushed too hard, numerical noise will dominated any corrected trace. So the measurements are close to being as good as can be expected.

Conclusion and Error Analysis

	Focal E(V/m)	y<0, z=0	E (V/m)	y>0, z=0	E (V/m)	y=0, z<0	E (V/m)	y=0, z>0	E (V/m)
2 Arm B-Dot	2.45	y=-2cm	2.27	y=2cm	2.01	z=-1cm	2.46	z=1cm	2.41
		y=-4cm	2.27	y=4cm	1.44	z=-2cm	**2.47**	z=2cm	2.40
		y=-6cm	1.15	y=6cm	0.97	z=-4cm	2.35	z=4cm	2.28
		y=-8cm	0.79	y=8cm	0.66	z=-6cm	2.21	z=6cm	2.18
						z=-8cm	2.03	z=8cm	2.07
						z=-10cm	1.80	z=10cm	1.95
						z=-12cm	1.57	z=12cm	1.69
						z=-14cm	1.30	z=14cm	1.48
						z=-16cm	1.12	z=16cm	1.38
4 Arm B-Dot	3.36	y=-2cm	2.95	y=2cm	2.56	z=-1cm	3.41	z=1cm	3.32
		y=-4cm	2.94	y=4cm	1.50	z=-2cm	**3.42**	z=2cm	3.27
		y=-6cm	1.02	y=6cm	0.94	z=-4cm	3.25	z=4cm	3.13
		y=-8cm	0.86	y=8cm	0.89	z=-6cm	2.90	z=6cm	3.01
						z=-8cm	2.65	z=8cm	2.85
						z=-10cm	2.35	z=10cm	2.69
						z=-12cm	2.26	z=12cm	2.35
						z=-14cm	1.85	z=14cm	2.09
						z=-16cm	1.52	z=16cm	1.93

Table 1: Eeq Values for x and z direction

One can see from table 1 that our focal point is close to reflector about 2 cm because we do not have enough high frequencies. If we compare the variation in x-direction they have to be same but they are different this is because the error in the geometric shape or alignment of prolate-spheroidal reflector.

	Analytic results(V/m)	Exp results(V/m)	Oscillation(V/m)	tmr(ps)	Error(%)
B-Dot 2Arm	3.25	2.5	0.4	119	21.4
B-Dot 4Arm	5.2	3.5	0.97	127	32.7
D-Dot 2Arm	3.25	2.5	0.38	119	21.4
D-Dot 4Arm	5.2	3.5	0.92	130	32.7
D-Dot 2Arm fast	14.8	9.6	1.58	26.5	35.1
D-Dot 4Arm fast	29	19.8	3.3	22	31.7

Table 2: Analytical, Experimental results, Oscillation Amplitude, t_{mr} and error in Experimental Results w.r.t Analytical Results

If we use the slow sensors, they are more sensitive than slow D-Dot sensor but they are not fast enough so we can not obtain the actual t_{mr} values. We obtain bigger t_{mr} values this causes decrease in the amplitude of the impulse of the focal waveform. If we use the fast D-Dot sensor, it is not sensitive enough so we obtain higher amplitudes in the impulsive part but we obtain more errors in the amplitude of the impulsive part of the focal waveform.

We have analytical and experimental errors. When the focal fields are calculated in [1] the aperture integral does not consider the feed arms and feed-arm thicknesses. This can cause an error in the calculation of the impulse amplitude of the focal waveform.

We have errors that are related with the experiments. We are in the limit of our instrumentation so we have less accuracy. We have checked the pulser and the connection cables and we have not found any problems. They are presented in fig 12.

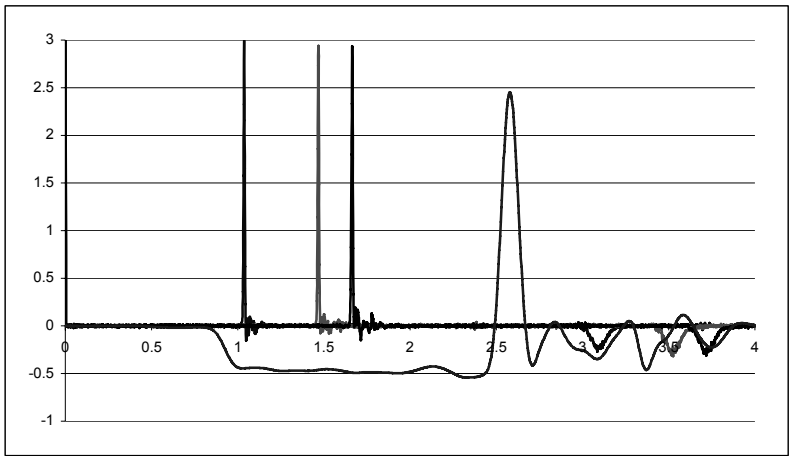

Figure 12: The Normalized data from the pulser, 2 nano second and 3 nano second long cable and the focal waveform

One can see from fig. 12 that the postpulse oscillations are not from the pulser, the 2 nano-second and 3 nano-second long cable that we use to connect the pulser to the feed arms and sensors to the sampling oscilloscope.

Then we checked the prepulse term and took the derivative of that

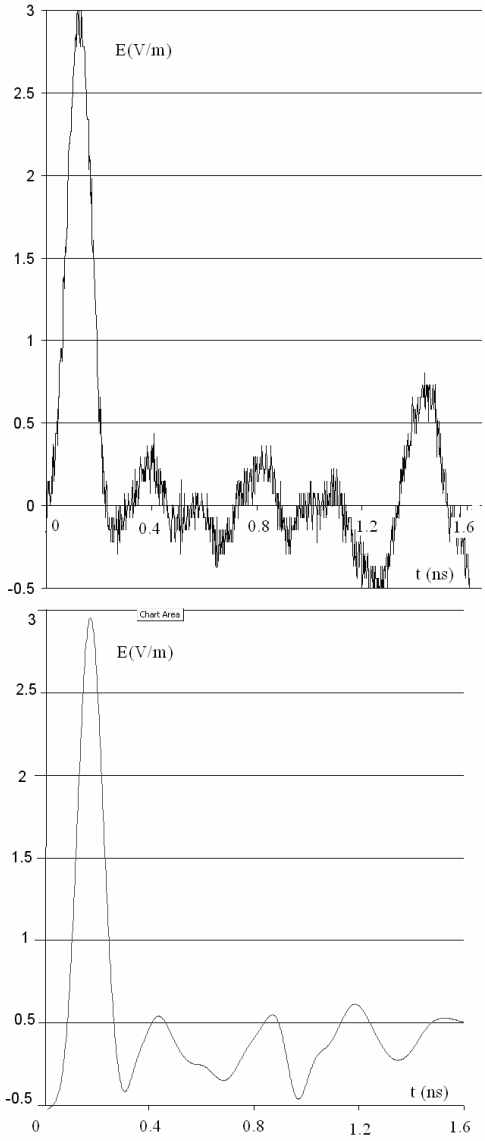

Figure 13: The derivative of the normalized prepulse term and the focal waveform

They are oscillating with similar frequencies so this proves that we have a problem between pulser and feed-arm connection. The ripples in the prepulse can not be associated with the feed arms near the reflector, by causality (speed of light).

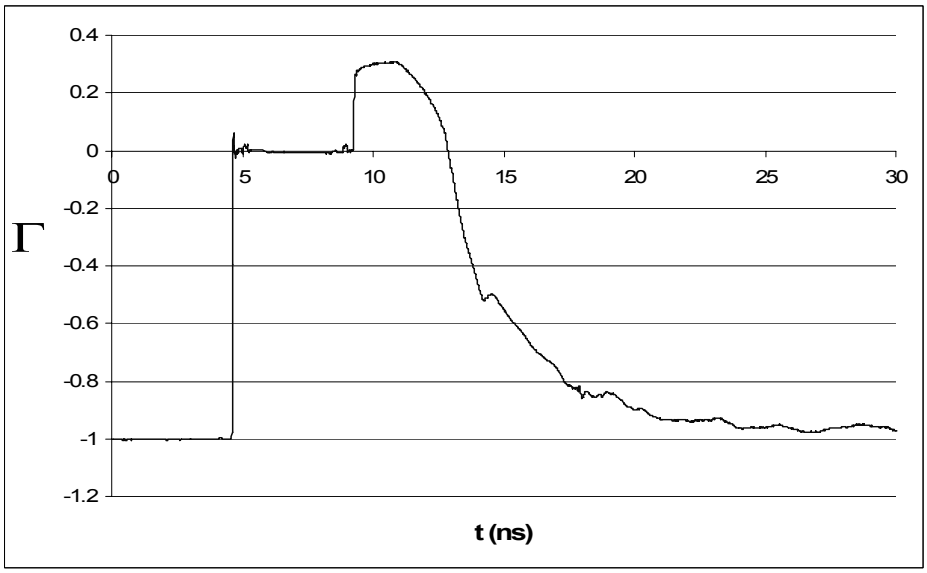

Figure 14: Reflection Coefficient (Γ)

One can see the reflection coefficient (Γ) values from fig. 14 . It starts from -1 as short circuit, it goes to 0 when the current reaches to $50\,\Omega$ cable , it goes to 0.3 when it reaches to the feed arms. Finally it goes to -1 because reflector feed arms are shortened. We can calculate the feed arms pulse impedance as follows $\Gamma = 0.3$

$$\Gamma = \frac{Z_L - Z_0}{Z_L + Z_0} \tag{9}$$

$\Gamma = 0.3$ so $Z_L = 93\ \Omega$ this impedance is close to the our analytical value of $Z_L = 100\ \Omega$ so we do not have any problem in the feed arms geometry.

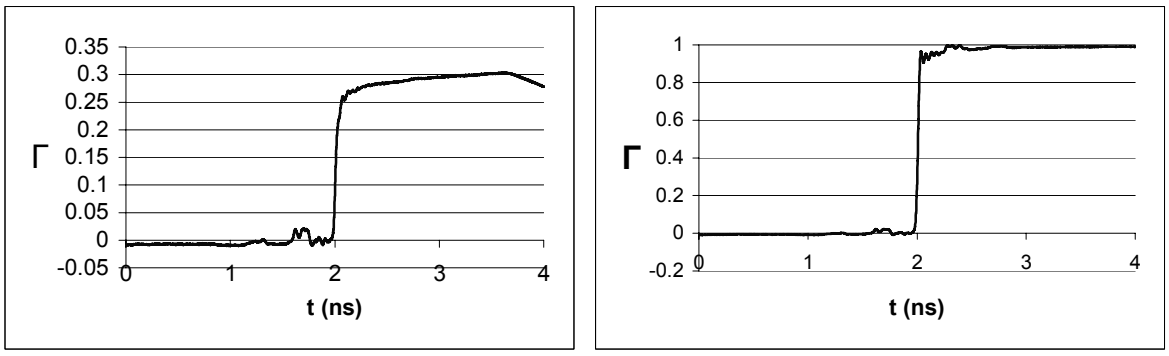

a) b)

Figure 15: Reflection Coefficient (Γ) a)with feed arms b)open circuit

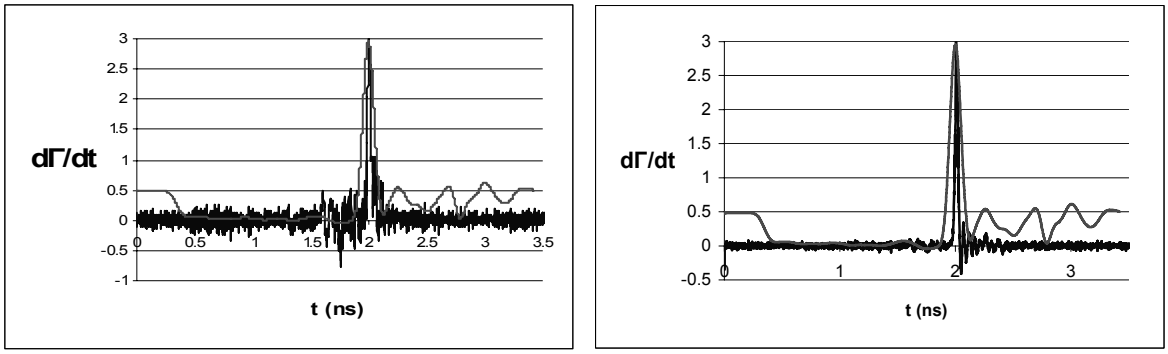

a) b)

Figure 15: Normalized derivative of Γ and focal waveform a)with feed arms b)open circuit

One can see from fig. 15 we have ripples in the Γ . If we compare the normalized derivative of the Γ with focal waveform for feed arms and open circuit case as presented in fig. 16, they are not oscillating in the similar frequencies so the transition between barrels may not cause these oscillations . Even we have perfect connection between feed arms and excitation point on the table, it is hard to get actual focal waveform because of geometric restriction problem.
One can see from fig. 11 B-dot sensor causes the ringing in the postpulse, but we could not find the reason that causes the difference between amplitude of the analytical and numerical results. We have analytical and experimental errors. When the focal fields are calculated in [1] the aperture integral does not consider the feed arms and feed-arm thicknesses. This can cause an error in the calculation of the impulse amplitude of the focal waveform, we believe this is the main error that can cause the inconsistency between analytical and experimental results.We have errors that are related with the experiments. We are in the limit of our instrumentation so we have less accuracy.

References

1. C. E. Baum, “Focal Waveform of a Prolate-Spheroidal Impulse-Radiating Antenna (IRA),” Radio Science , accepted for publication .
2. S.Altunc and C.E.Baum. “Extension of the Analytic Results for the Focal Waveform of a Two-Arm Prolate-Spheroidal Impulse-Radiating Antenna (IRA)”, Sensor and Simulation Note 518, Nov 2006.
3. K. H. Schoenbach, R. Nuccitelli and Stephen J. Beebe, “ZAP”, IEEE Spectrum, Aug 2006, Pg 20-26.